Please cite this article in press as: De Bastiani et al., Bifacial perovskite/silicon tandem solar cells, Joule (2022), https://doi.org/10.1016/j.joule.2022.05.014

Joule

CellPress

Perspective

Bifacial perovskite/silicon tandem solar cells

Michele De Bastiani,[1,2,*] Anand S. Subbiah,[1] Maxime Babics,[1] Esma Ugur,[1] Lujia Xu,[1] Jiang Liu,[1] Thomas G. Allen,[1] Erkan Aydin,[1] and Stefaan De Wolf[1,*]

SUMMARY

Perovskite/silicon tandem solar cells are a rapidly emerging class of high-efficiency photovoltaic (PV) devices that have demonstrated excellent power conversion efficiencies (PCEs) while promising low-cost manufacturing. In recent years, this technology has been pushed increasingly closer to market entrance. Yet, for true commercial success, PCEs also need to be stable, in line with the warranty certificates of commercial crystalline-silicon (c-Si) PV modules. Bifacial tandem solar cells that collect light at both their sunward and rear side by exploiting the albedo—the scattered and reflected photons from the ground—offer a promising pathway toward a greater stability and energy yield. Thanks to the additional photons arising from the albedo, bifacial solar cells may generate a current larger than their conventional monofacial counterparts, enabling a higher performance. For bifacial monolithic tandems, exploiting such current enhancement requires current matching between top and bottom cells, which mandates the use of a bromide-lean, narrow-band-gap perovskite that is known to suppress halide segregation, thereby significantly improving device stability. In this perspective, we discuss bifacial perovskite/silicon tandem technology in depth, highlighting its great appeal, thanks to its combination of enhanced performance and improved stability with promising low costs, thereby representing a key future technology at the utility scale that can contribute to the formation of a carbon-neutral sustainable economy.

INTRODUCTION

Bifacial solar cells refer to a particular device architecture designed to absorb light simultaneously from both the front side (sunward) and rear side of the device.[1] Solar irradiation at the rear side originates from the albedo, i.e., the reflected and scattered light from the ground.[2] Thanks to the extra photons arising from the absorbed albedo, bifacial solar cells can generate higher current densities above the limits of conventional (monofacial) device configurations.[3] This gain in current density directly translates into a higher power output. As a result, the bifacial configuration is rapidly taking a prominent market position among mainstream single-junction crystalline-silicon (c-Si) photovoltaic (PV) technologies.[4] Indeed, a growing number of manufacturers are now offering bifacial modules, particularly aimed at the utility-scale market.[5] The gain in performance due to bifaciality is proportional to the intensity of the albedo.[6,7] Therefore, highly reflective ground surface materials such as sand, concrete, and snow are preferred for such bifacial PV systems.[2]

Recently, the emergence of band-gap-tunable perovskite solar cells (PSCs) has stimulated significant interest in tandem applications—particularly the perovskite/silicon

Context & scale

Thanks to their remarkable power conversion efficiencies, perovskite/silicon tandems hold great promise to generate sustainable electricity at the terawatt scale. However, to succeed in this challenge, these tandems need to overcome the performance instability challenge, a phenomenon often still pestering perovskite-based solar cells. Here, we review the potential of bifacial perovskite/silicon tandem solar cells to simultaneously improve the performance and stability of perovskite-based devices. The bifacial configuration capitalizes on extra photons originating from reflected and scattered light from the ground. To translate this into increased performance, a reduction in the band gap of the perovskite sub-cell is required. Indeed, conventional tandems require specific mixtures of iodide and bromide for an optimal band gap, which often result in undesirable halide segregation and device failure under operational conditions when the bromide-to-iodide ratio is high (as is the case for wide-band-gap perovskites). Conversely, the narrower perovskite band gap required for bifacial perovskite/silicon tandems allows for a bromide-lean composition, suppressing halide segregation, which simultaneously enhances the performance and stability relative to monofacial perovskite/

tandem implementation—as a future mainstream PV technology.[8–11] Several studies have already indicated that the gain in performance of such tandems may positively pay back their higher manufacturing costs, especially in the monolithic configuration, where the perovskite sub-cell is directly fabricated atop of the c-Si bottom cell, resulting in a two-terminal device.[12,13] The record power conversion efficiency (PCE) of perovskite/silicon tandems is already approaching 30%, which is higher than the theoretical single-junction limit for c-Si solar cells, thereby offering promising perspectives for a very-high-performance commercial PV technology.[14] However, the instability in the performances of contemporary PSCs still raises significant concerns about their commercialization, even more so when considering the ever-increasing warranties given for c-Si modules for stable outdoor performance (beyond 30 years now for some manufacturers).[15,16] Such high stability standards may be a particular challenge when relatively large perovskite band gaps (generally >1.68 eV) are required, which, for instance, is the case in the monolithic tandem configuration. Indeed, for these monofacial devices, the perovskite band gap needs to be sufficiently large to enable current matching between the two sub-cells.[17] Generally, this is accomplished by increasing the bromide-to-iodide ratio in the perovskite composition. Yet, a too high ratio leads to halide segregation, especially under light exposure, contributing to device instability.[18] In the bifacial perovskite/silicon tandem configuration, the additional current gain in the silicon sub-cell due to the absorbed albedo mandates a reduction in the perovskite band gap, even toward bromide-free compositions, simultaneously improving both the device performance and stability.[15] For this reason, more than any other PV technology, perovskite/silicon tandems can benefit from bifaciality.[19] In this perspective, we review the key characteristics of bifacial perovskite/silicon tandems and provide direct insights into the correlation between the perovskite band gap, current generation in the tandem, the albedo, and halide segregation. Later, we elucidate the challenges for the fabrication of bifacial tandems as well as their performance characterization and power rating in the controlled lab environment. Finally, we argue how bifaciality is expected to play a pivotal role in the successful commercialization of perovskite-based solar cells.

silicon tandems. Based on these considerations, we review here the peculiar characteristics of bifacial perovskite/silicon tandem technology and address the challenges related to the characterization of this unique class of devices. We conclude by providing insights into photovoltaic industry trends and how bifacial perovskite/silicon tandem solar cells may take the leading market position in the near future.

CURRENT MATCHING AND BIFACIALITY

In a monolithic monofacial tandem, the two sub-cells are connected atop each other in series via a recombination junction.[20] Therefore, the voltage output of a tandem device is the sum of the individual sub-cell voltages, whereas the current output is limited by the lowest current among the two (Figure 1A).[21] The highest tandem performance is achieved when the two sub-cells generate high, identical current densities (resulting in the so-called current matching condition).[22,23] In perovskite/silicon tandems, current matching is obtained through adequate optical device design, which includes tailoring of the perovskite band gap, refractive index matching of materials, as well as minimizing external light reflection and parasitic optical absorption.[24,25] When the current generated is higher in one sub-cell than in another, the tandem is in a current-mismatched condition. Usually, the fill factor (FF) of the tandem then increases, resulting in a partial compensation for the loss in performance caused by the reduced current, as well described by Köhnen et al.,[21] Boccard et al.,[26] and Onno et al.[27] A bifacial tandem is purposely designed for its top cell (the perovskite) to generate more current than the filtered bottom cell (the silicon), when only considering sunward illumination.[19,27] Yet, with a rear transparent electrode, the bottom cell can also absorb light reflected from the ground and generate additional bottom-cell current. This can compensate for the limited bottom-cell current generated by photons only from the sun side, reestablishing

[1]KAUST Solar Center (KSC), Physical Sciences and Engineering Division (PSE), King Abdullah University of Science and Technology (KAUST), Thuwal 23955-6900, Kingdom of Saudi Arabia

[2]Present address: Department of Chemistry & INSTM Università di Pavia, Via T. Taramelli 14, Pavia 27100, Italy

*Correspondence: michele.debastiani@kaust.edu.sa (M.D.B.), stefaan.dewolf@kaust.edu.sa (S.D.W.)

https://doi.org/10.1016/j.joule.2022.05.014

Please cite this article in press as: De Bastiani et al., Bifacial perovskite/silicon tandem solar cells, Joule (2022), https://doi.org/10.1016/j.joule.2022.05.014

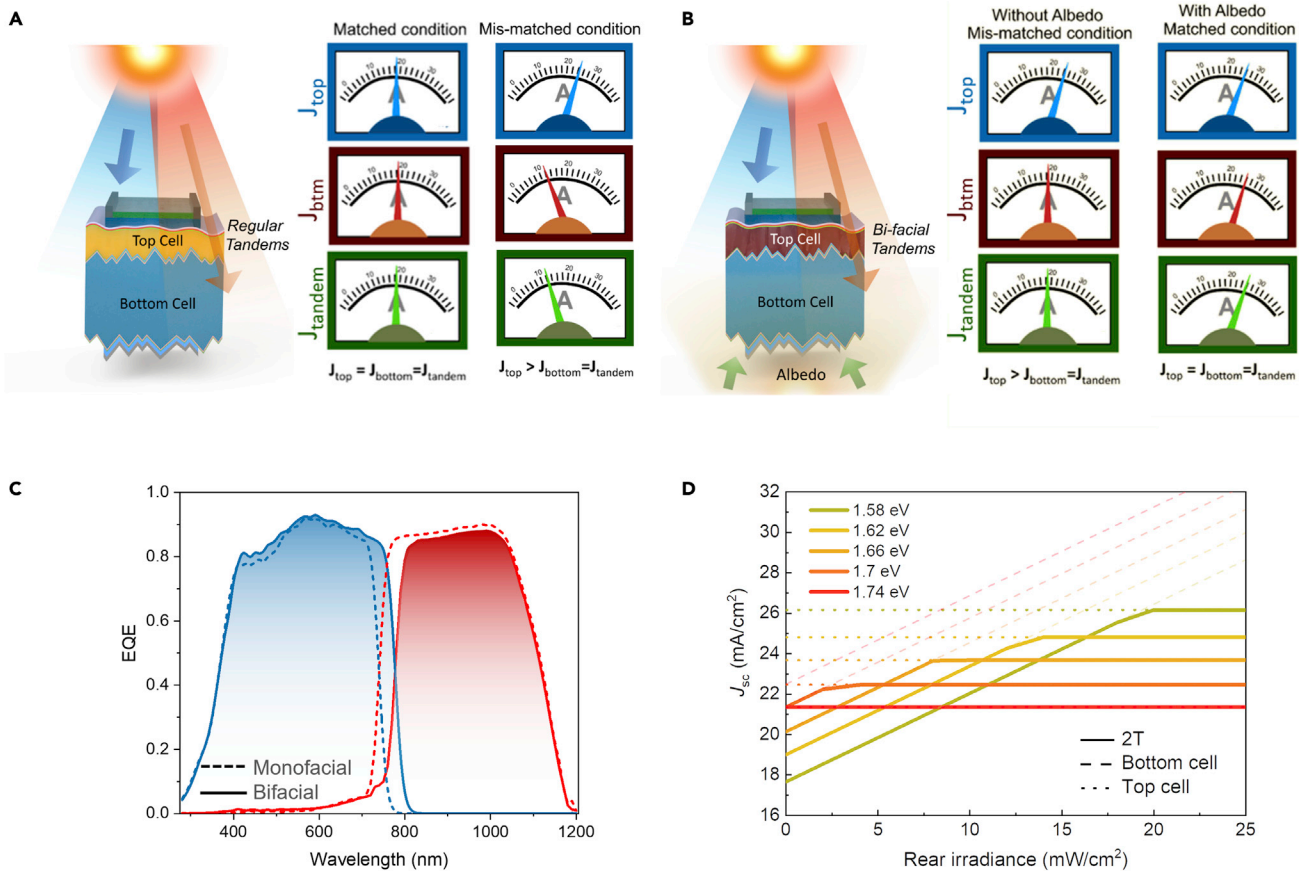

Figure 1. Current-density (J) generation for monofacial and bifacial tandems

(A) Current output for a conventional (monofacial) tandem in conditions that are current matched and mismatched.

(B) Current output for a bifacial tandem without and with albedo. With albedo, the current generated by the bifacial tandem is higher than the current of a current-matched monofacial tandem. The blue arrow represents the light absorbed by the top cell, whereas the red arrow represents the light absorbed by the bottom cell. The albedo is represented at the rear of the bifacial tandem.

(C) External quantum efficiency (EQE) of a monofacial (dashed line) and bifacial tandem (full line). The blue part and red part represent the current generated by the perovskite sub-cell and the silicon sub-cell, respectively. Figure adapted from De Bastiani et al.[19]

(D) J_{sc} contributions from the individual sub-cells (dashed and dotted lines) and the overall tandem cell (solid lines) for different top-cell band gaps as a function of rear irradiance.

current matching (Figure 1B). As a result, the overall tandem current increases, directly translating into an enhanced performance. The external quantum efficiencies (EQEs) shown in Figure 1C provide a direct visualization of the different currents generated by each sub-cell, for both the monofacial and the bifacial tandems, as the current equals integration of the EQE over the solar spectrum. Hence, from the EQEs it is possible to predict the maximum current generated by the bifacial tandem in the presence of the appropriate amount of extra photons at the rear side. To highlight the correlation between the top-cell band gap and the rear irradiance, we computed the short-circuit current density, J_{sc}, of bifacial monolithic tandems (details in the supplemental information) as a function of the top-cell band gap and rear irradiance. In the simulation, we modeled the absorption in both cells as a step function determined by the band-gap energy, as is typical for radiative limit calculations for arbitrary band gaps. For the bottom cell, we fixed the band-gap value to 1.12 eV. The J_{sc} simulations are displayed in Figure 1D and are augmented with an additional rear irradiance of 25 mW/cm^2, which is a realistic upper limit value for the albedo in outdoor operational conditions.[17,19,28] In the case of a top-cell band gap

Please cite this article in press as: De Bastiani et al., Bifacial perovskite/silicon tandem solar cells, Joule (2022), https://doi.org/10.1016/j.joule.2022.05.014

of 1.74 eV, we found that the rear irradiance albedo does not enhance J_{sc} of the tandem as the current density is always limited by the top cell. However, reducing the top-cell band gap allows the rear irradiance to increase the two-terminal J_{sc}. Notably, for a given top-cell band gap, the J_{sc} saturates at specific values of the rear irradiance. This saturation indicates that current matching is reached for that specific band gap; the only way to benefit from an even stronger albedo would be by further decreasing the top-cell band gap.

To properly describe the characteristics that define bifacial solar cells, we here clarify the terminology often used to report on their performances. The *albedo* (adimensional) is defined as the ratio between the diffuse reflections from the ground with respect to the direct front irradiation:

$$albedo = \frac{the\ reflected\ light\ (\mathrm{mW/cm^2})}{the\ incident\ light\ (\mathrm{mW/cm^2})}$$

Often it is useful to describe the power provided by the photons arising from the albedo with the term *rear irradiance* (in $\mathrm{mW/cm^2}$). Both the albedo and the spectrum of the rear irradiance depend on the ground material. It follows that the *effective albedo* is defined as the spectral component of the albedo that can be absorbed by the bottom cell, generating extra current (for c-Si solar cells, for example, the relevant spectral range is up to 1,200 nm).[29] Lehr et al. simulated the change in energy yield of bifacial tandem installations for different ground covering materials[2]; obviously, materials with a high reflection and high effective albedo are preferred to maximize a bifacial cell's energy output. To fully describe bifacial performance, two more definitions are needed. The *bifaciality* (BiFi) *factor* is used for single-junction solar cells only; it is the ratio between the power generated when the solar cell is irradiated in monofacial mode from the front side and rear side, using a non-reflecting measurement stage (usually coated black).[30,31] For monolithic and bifacial tandems the BiFi factor is a meaningless metric, as neither of these cell architectures generate power when light is coming in from the rear side (monofocal tandems generate no current in the bottom cell due to the full opaque rear metallization, whereas in the bifacial tandem the top cell is in an open circuit, resulting in no current output when only the rear side is illuminated). Alternatively, the BiFi factor is a useful term to represent the power generation of bifacial devices (tandem or single junction) under specific rear irradiation, usually expressed as a subscript in $\mathrm{W/m^2}$. For example, a power generation density (PGD) of 25 $\mathrm{mW/cm^2}$ $\mathrm{BiFi_{200}}$ means that the 25 mW are generated per $\mathrm{cm^2}$ of device area, when the device is simultaneously subjected to 1-sun irradiance at the front (1,000 $\mathrm{W/m^2}$) and 0.2-sun irradiance (200 $\mathrm{W/m^2}$, denoted as $\mathrm{BiFi_{200}}$) at the rear.[32] Moreover, we note that the conventional use of PCE to describe the performance of solar cells is meaningless for bifacial configurations. Indeed, PCE is defined as the ratio of the power output of the device over the incident power from the irradiation, over a given surface area. Since the total irradiation to which a bifacial device is subjected, in the presence of the albedo, is more than 1-sun per unit device area, the correct way to report the bifacial performance is by using the BiFi factor. Table 1 summarizes these definitions.

Finally, we clarify the difference between *bifacial* (single-junction or tandem) solar cells and *semi-transparent* solar cells. Both devices feature a transparent, rather than an opaque, back electrode. However, bifacial devices aim to maximize the absorption of photons both at the sun side and rear side and find application mostly in high-yield PV installations at the utility scale. Currently, the leading bifacial technology is c-Si based, with a few exploratory attempts employing thin-film technologies other than PSCs. Indeed, PSCs offer ideal conditions for the bifacial configuration, as

Please cite this article in press as: De Bastiani et al., Bifacial perovskite/silicon tandem solar cells, Joule (2022), https://doi.org/10.1016/j.joule.2022.05.014

Table 1. Definitions for bifacial solar cells and tandems

Term	Definition	Unit	Note
Albedo	ratio between the reflected and the front irradiation	adimensional	range from 0–1 0: perfect absorptive ground 1: perfect reflective ground
Effective albedo	the spectral component of the albedo that is absorbed by the rear of the bifacial cell (or sub-cell for the tandem) and that contributes to enhance the current	–	–
Rear irradiance	expression in power density to quantify the extra photons from the albedo	mW/cm^2	–
Bifaciality factor	ratio between the rear and the front performances of a bifacial solar cell, measured in monofacial configuration	%	not valid for bifacial tandems
BiFi factor	parameter used to report the power generation of a bifacial cell (or tandem) at a specific rear irradiance	W/m^2	–

demonstrated by several pioneering works and a constant growing interest.[33–37] Conversely, semi-transparent devices aim to absorb only a fraction of the visible incident light, leaving a transmitted component through it. In single-junction devices, this is achieved either by limiting the absorption range or the thickness of the photo-absorber material; alternatively, local openings may be present, resulting in color-neutral semi-transparency.[38] Perovskite and organic PVs (OPVs) and other thin-film solar cells such as amorphous silicon (a-Si) are the main technologies used for semi-transparent PV, with applications in building-integrated PV, among others.[39–43]

DESIGN OF THE DEVICE

Monolithic perovskite/silicon tandems are typically fabricated using either double-side textured or front-side polished silicon wafers. For both substrate types, the perovskite absorber can be deposited via solution. In the first case, the perovskite fills the spaces within the textured bottom cell surface (referred to here as the "levelized" configuration); in the second case, the perovskite crystallizes evenly on the polished surface (hereafter referred to as the "flat" configuration). Alternatively, the perovskite can also be processed on the textured surface via vacuum deposition, resulting in a conformal deposition (the "conformal" configuration), as Figure 2 depicts. Although bifacial perovskite/silicon tandems can be realized in each of these configurations, so far they have been reported only with the levelized configuration.[19] Each configuration has unique features and challenges for its fabrication: for example, the flat configuration offers the easiest perovskite deposition (similar to the deposition process used on glass substrates, except for the waviness of the wafer) but has the highest reflection; the levelized configuration reduces the reflection losses but makes the deposition of the layers on top of the silicon pyramids more complicated (particularly for polymeric transport layers); and the conformal configuration offers the most elegant optics, with the potential for record current generation. In the latter, however, it requires vacuum deposition of the perovskite, either by thermal evaporation or hybrid deposition (thermal evaporation coupled with a solution conversion step); both these techniques present the typical challenges of vacuum deposition: quality of the film, precise control of the co-evaporation (two to four sources), thickness control (only hybrid), and conversion control (only hybrid). It is not unlikely that in the next few years new deposition techniques will be reported (chemical vapor conversion, sputtering, pulsed laser deposition, inkjet printing, spray coating, etc.), enabling new configurations and possibly overcoming existing limitations. The fabrication of a bifacial

Please cite this article in press as: De Bastiani et al., Bifacial perovskite/silicon tandem solar cells, Joule (2022), https://doi.org/10.1016/j.joule.2022.05.014

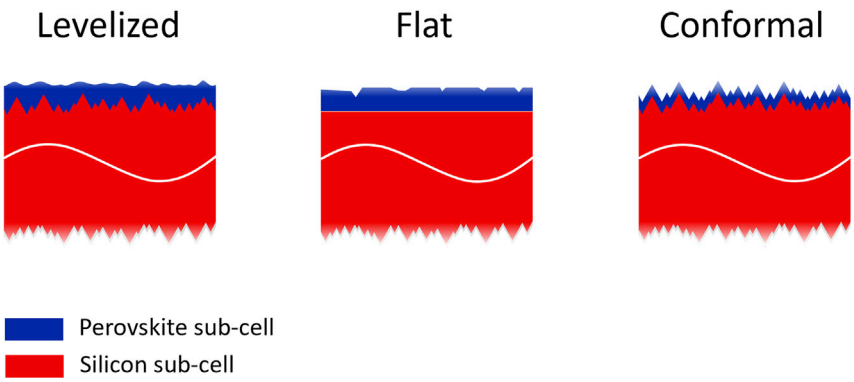

Figure 2. The different configurations of perovskite/silicon tandems

The tandems can be fabricated with textured and flat bottom cells. For clarity, only the perovskite and silicon absorbers are represented in blue and red, while all the other device layers are not shown.

perovskite/silicon tandem significantly differs from that of conventional monofacial tandems (Table 2). For example, for the levelized and flat configurations, the optimal perovskite band gap for monofacial tandems is between 1.65 and 1.70 eV;[23,44] yet, in the bifacial case, the perovskite band gap must be tailored to lower values ranging from 1.50 to 1.65 eV, depending on the rear irradiance intensity.[2,11,19] This smaller band gap allows the bifacial tandem to be current matched under actual outdoor operational conditions.

The typical perovskite structure is ABX_3. For metal halide perovskites, A and B are cations; A is either a small molecule (such as methylammonium, MA^+, and formamidinium, FA^+) or a large atom (such as Cs) placed in the octahedral lattice cages, B is a metal (such as Pb or Sn), and X is a halogen (mostly I and Br). Controlling the perovskite band gap is mostly achieved by tailoring the halogen composition (to a lesser extent this can also be accomplished by optimizing the A-site cation in the perovskite lattice), since the $(BX_6)^{4-}$ octahedral network determines the electronic and optical properties of the material.[45] It is also possible to tailor the band gap to lower values by replacing Pb with Sn at the B-site, even though this may make the material prone to oxidation-related degradation.[46] For high, yet realistic, albedo values (0.15–0.25), the ideal band gap is between 1.50 and 1.58 eV, allowing for bromide-free and thus highly stable perovskite compositions, as discussed in the next section.[2] Therefore, detailed knowledge of the albedo at the location of the PV installation is paramount for system design toward the highest energy yields. Moreover, to maximize the absorption of the albedo, the rear contact of the silicon subcell must be highly transparent, mandating a transparent rear contact stack with minimal parasitic absorption and minimized shading by its metal-grid electrode, requiring similar considerations as the front contact for single-junction devices.[47] In this direction, there are also important considerations for the module design, similar to the bifacial single-junction configuration, which has been the subject of extensive studies.[4,5]

From a research perspective, the fabrication of the c-Si bottom cell for bifacial perovskite/silicon tandems requires a few additional points of attention, compared with monofacial tandems. In particular, the device's rear must be protected during the complete processing sequence to avoid unwanted material deposition or damaging the fragile pyramidal c-Si structure of the rear contact. In our experience, the optimal fabrication for the bottom cell starts with the wafer preparation. This step includes

Please cite this article in press as: De Bastiani et al., Bifacial perovskite/silicon tandem solar cells, Joule (2022), https://doi.org/10.1016/j.joule.2022.05.014

Table 2. Differences between the monofacial and bifacial configuration of perovskite/silicon tandem solar cells

	Monofacial	Bifacial
Sun-side contact	optimized for current matching, depending on the perovskite band gap.	maximized for perovskite current output, depending on the albedo conditions.
Perovskite	band gap: 1.63–1.65 eV for textured configuration. 1.65–1.70 eV for levelized configuration.	band gap: 1.50–1.65 eV, depending on the albedo conditions.
Rear-side contact	optimized for light coupling in the near-IR, spaced reflector. Opaque electrode.	optimized for low-irradiance and high transparency according to effective albedo.

saw-damage removal and texturing, usually accomplished in alkaline solutions. After that, the wafers are cleaned with standard wafer cleaning procedures (often called SC1 and SC2) to remove organic and metal contaminants. Subsequently, the passivating layers and doped layers (acting as charge-selective layers), typical of silicon heterojunction (SHJ) solar cells, are deposited by plasma-enhanced chemical vapor deposition (PECVD). Next, transparent conductive oxides (TCOs) are sputtered onto the front and rear side using physical vapor deposition (PVD), usually via sputtering. The front TCO acts as part of the recombination junction of the tandem, whereas the rear TCO is optimized for the device to absorb albedo photons (this optimization includes the thickness, the carrier density, and the mobility of the TCO). After this step, a silver grid is screen printed on the rear TCO and annealed to cure the metal paste and relieve sputter damage. Next, the cells are scribed by a laser (mainly for lab-sized samples, one wafer usually accommodates several bottom cells; for industrial-sized tandems, this step is skipped as the tandem has then the same dimensions of the wafer). Prior to the last step, the rear contact of the bottom cell is covered by a protective film to avoid physical damage during the perovskite top-cell fabrication. The complete bottom-cell process is shown in Figure 3.[15,19]

From an industrial perspective, the difference between the monofacial and bifacial tandems is less pronounced than in the research environment. Certainly, the bifacial tandems will largely benefit from the well-established knowledge of bifacial silicon modules, coupled with the state-of-the art monolithic tandem fabrication (either vacuum or solution processed). Furthermore, the rear contact that is designed for maximizing the absorption of the albedo is similar to the rear contact of bifacial c-Si heterojunction solar cells. This contact encompasses a TCO with minimized optical losses and a screen-printed metal grid for the rear terminal. For the perovskite deposition, the lower band gap of the tandem (ideally bromide free) simplifies the deposition process, reducing the number of components in the ink formulation or the number of sources for the co-evaporation process. Moreover, with the high level of automation typical of production lines, the protection of the rear contact during the perovskite deposition will most likely not be required.

IMPACT ON STABILITY

Besides featuring excellent optoelectronic quality, control of the band gap is one of the most important properties for a semiconductor to be of interest for tandem applications. The band gap of perovskites can be tailored through their chemical composition, particularly via tuning the electronegativity between the metal-halogen bonding in the crystal lattice. Practically, in halide perovskites, the tailoring of the band gap is achieved by simply controlling and optimizing the precursors in the solution before deposition or by controlling the deposition rates in vacuum processing.[48–50] Tuning the perovskite band gap is part of the current-matching strategy, which is required for efficient tandem design. The desired band gap depends on the optics and the architecture of the tandem. Indeed, for monofacial monolithic

Please cite this article in press as: De Bastiani et al., Bifacial perovskite/silicon tandem solar cells, Joule (2022), https://doi.org/10.1016/j.joule.2022.05.014

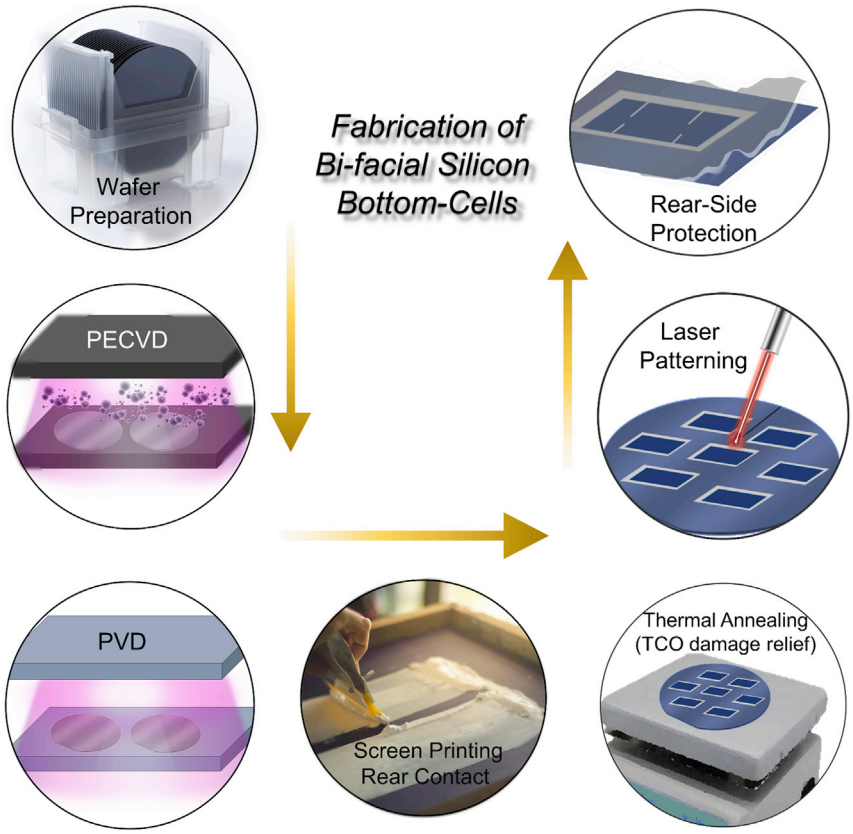

Figure 3. The fabrication steps of a bifacial silicon bottom cell

The first three parts are shared with the fabrication of monofacial bottom cells, although the layers deposited via physical vapor deposition (PVD) and plasma-enhanced chemical vapor deposition (PECVD) may be different, especially in view of minimizing parasitic optical absorption. The thermal annealing has the double function of curing the rear contact and relieving the PVD damage caused to the amorphous silicon. The laser patterning and scribing are typical for lab-scale devices, where one silicon wafer can accommodate several bottom cells. However, the new trends of using half-cut cells employ a similar process.

tandems with a textured bottom cell and conformal perovskite, the optimal perovskite band gap lies between 1.63 and 1.65 eV. The perovskite band gap widens from 1.65 to 1.7 eV for monofacial monolithic tandems with flat or levelized perovskite top cells (see also Table 2). The conformal configuration significantly reduces the reflection losses, allowing for a reduction in the perovskite band gap in favor of higher current outputs. In contrast to this, flat or levelized configurations are more prone to external reflection losses and therefore require the broadening of the perovskite band gap—with a bromide content beyond ~20% needed to achieve current matching. Unfortunately, with such large amounts of bromide, the perovskite is affected by the phenomenon of (light-induced) halide segregation whereby iodide and bromide separate under operational conditions into iodide-rich and bromide-rich phases.[18] Consequently, this changes the optoelectronic properties of the perovskite, leading to rapid degradation in device performance. Figure 4A shows the time evolution of the photoluminescence (PL) for a perovskite film ($Cs_{0.5}MA_{0.15}FA_{0.8}Pb(I_{0.75}Br_{0.25})_3$, band gap of 1.68 eV) under constant irradiation at 1-sun for 45 min. The PL shifts in position and broadens in shape, suggesting that the halogen composition is changing. Passivation strategies in the bulk and at the grain boundaries and surfaces must be used to minimize this deleterious effect.[8,23,44] Figures 4B

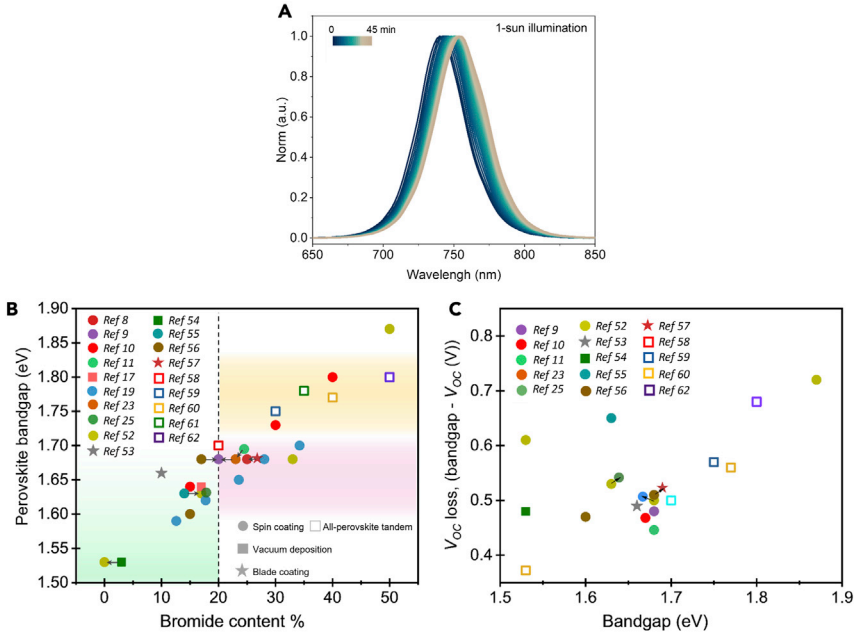

Figure 4. The band gap in perovskite-based tandems

(A) Evolution of the photoluminescence over 45 min of a 1.68 eV $Cs_{0.5}MA_{0.15}FA_{0.8}Pb(I_{0.75}Br_{0.25})_3$ film under constant irradiation at 1-sun condition.

(B) The perovskite band gap as a function of the bromide content for tandem applications. The perovskites reported here vary in the A-site cation composition as well, influencing both the band gap and stability. The pink, green, and yellow backgrounds represent the band gaps and bromide content for monofacial tandems, bifacial tandems, and all-perovskite tandems, respectively. The dashed line represents the % of bromide where halide segregation becomes likely. Data are edited from the respective publication reported as a reference in the caption. For comparison, we report also the complete composition of the perovskite. Jacobsson et al.[51] $[MA_{16.6}FA_{83.3}Pb(I_{1-x}Br_x)_3]$; De Bastiani et al.[19] $[Cs_5MA_{14}FA_{81}Pb(I_{1-x}Br_x)_3]$; Xu et al.[10] $[Cs_{25}FA_{75}Pb(I_{1-x}Br_x)_3]$; Al-Ashouri et al.[11] $[Cs_5(FA_{77}MA_{0.23})_{0.95}Pb(I_{77}Br_{23})_3]$; Kim et al.[9] $[Cs_{0.15}MA_{0.2}FA_{0.65}Pb(I_{0.8}Br_{0.2})_3]$; Chen et al.[52] $[Cs_{0.1}MA_{0.9}Pb(I_{0.9}Br_{0.1})_3]$; Aydin et al.[17] $[Cs_{25}FA_{75}Pb(I_{83}Br_{17})_3]$; Isikgor et al.[23] $[Cs_{15}MA_{15}FA_{70}Pb(I_{80}Br_{20})_3]$; Roß et al.[53] $[MA_{0.5}FA_{0.63}PbI_{3.13}]$; Bush et al.[54] $[Cs_{17}FA_{83}Pb(I_{83}Br_{17})_3]$; Mazzarella et al.[25] $[Cs_{0.05}MA_{0.16}FA_{0.79}Pb(I_{0.82}Br_{0.18})_3]$; Hou et al.[8] $[Cs_{0.05}MA_{0.15}FA_{0.8}Pb(I_{0.75}Br_{0.25})_3]$; Zhumagali et al.[55] $[Cs_{0.15}MA_{0.15}FA_{0.70}Pb(I_{0.80}Br_{0.20})_3]$; Subbiah et al.[56] $[MAPb(I_{0.75}Br_{0.25})_3]$; Palmstrom et al.[57] $[Cs_{0.3}DMA_{0.1}\ FA_{0.6}Pb(I_{0.8}Br_{0.2})]$; Zhao et al.[58] $[Cs_{0.2}FA_{0.8}Pb(I_{0.7}Br_{0.3})_3]$; Lin et al.[59] $[Cs_{0.2}FA_{0.8}Pb(I_{0.6}Br_{0.4})_3]$; Yu et al.[60] $[Cs_{0.4}FA_{0.6}Pb(I_{0.65}Br_{0.35})_3]$; Eperon et al.[61] $[Cs_{0.17}FA_{0.83}Pb(I_{0.5}Br_{0.5})_3]$.

(C) The voltage losses of the perovskite top cell (or top-cell analog were available, calculated as the perovskite band gap minus the open-circuit voltage) as a function of the perovskite band gap for both perovskite/silicon and all-perovskite tandems.

and 4C show the perovskite band gap as a function of the bromide content (in % with respect to the total halogen composition) for different publications related to perovskite-based tandem applications. To provide a complete perspective, we have also included tandems based on two perovskite absorbers (i.e., perovskite/perovskite tandems). The red region represents the compositions suitable for monofacial tandems, the green region those for bifacial tandems, and the yellow region those for all-perovskite tandems (here, only reporting the wide-band-gap perovskite needed for the top cell; the narrow-band-gap perovskite for the bottom cell has its own stability challenges, mainly related to the presence of Sn). The dashed line represents the bromide threshold: perovskites with higher bromide contents suffer from segregation and stability issues. In the green region, the bromide content is minimal, and the threat of halide segregation is significantly reduced. A high bromide content in the perovskite film affects not only the stability but also the performance. Indeed, Figure 4C shows the voltage loss (calculated as the perovskite band

Please cite this article in press as: De Bastiani et al., Bifacial perovskite/silicon tandem solar cells, Joule (2022), https://doi.org/10.1016/j.joule.2022.05.014

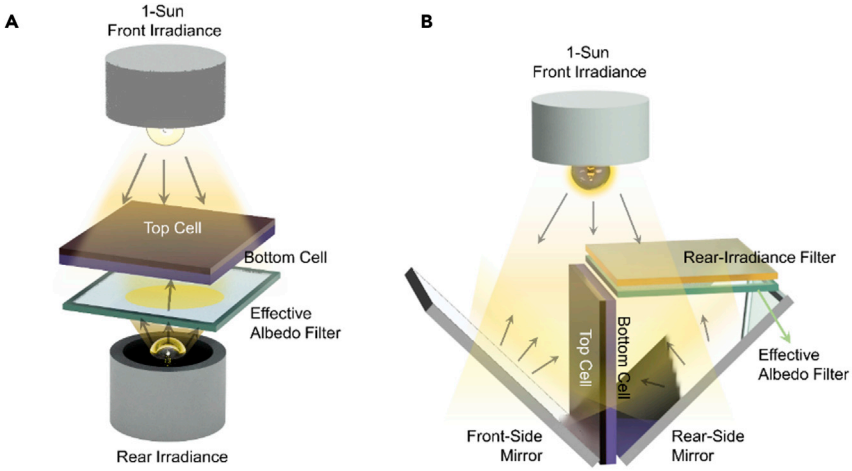

Figure 5. Characterization of bifacial tandem

Two possible setups for the characterization of the bifacial tandem.

(A) Double light sources, with the sun-side light fixed at 1-sun, whereas the rear-side light is variable to simulate different rear irradiances. Spectral filters can be applied at the rear to simulate specific effective albedos.

(B) Single light source, with the bifacial tandem in between two mirrors forming an angle of 45° with the device. The light source is fixed at 1-sun, while intensity filters and spectral filters are applied at the rear-side mirror to simulate different rear intensities and effective albedos, respectively. It is important to note that the sun-side irradiation must meet all the requirements for tandem characterization, particularly for the spectral response.

gap minus the open-circuit voltage) as a function of the perovskite band gap for many of the perovskite compositions shown in Figure 4B. Most of the monofacial tandems with 1.68 eV perovskite band gap have voltage losses between 0.4 and 0.5 V, whereas perovskite band gaps higher than 1.70 eV, including bromide content >20%, have higher voltage losses, losing a large part of the benefit of a wider band-gap semiconductor. Table S1 summarizes the data in Figure 4B, and the data for Figure 4C is presented in the supplemental information.

Recently, we have reported on the outdoor performances of a bifacial tandem following a 6-month investigation.[15] The bifacial tandem employed a 1.59 eV band-gap perovskite with minimized bromide content. During this period, we found that the main degradation of the device was related to alterations in the tandem's contacts and not so much to its bulk. Indeed, the optoelectronic properties of the tandem were mostly preserved. Particularly, the PL and output voltage, after prolonged outdoor measurements, showed the same characteristics of the initial condition.

CHARACTERIZATION OF BIFACIAL TANDEMS

Another challenge in researching bifacial tandems is the need for an adequate current density-voltage (*JV*) characterization setup, which must include the option of accurate control of the rear irradiance. Figure 4 shows two possible setups. The first case relies on two light sources: one at the sun side (simulating the AM1.5 spectrum) and one at the rear side (simulating the effective albedo [Figure 5A]). The intensity of the rear light varies to obtain the desired rear irradiance, whereas the sunward illumination is fixed at typical AM1.5G 1-sun conditions. Spectral filters can be applied at the rear side to simulate the effective albedo, for example, to mimic different ground materials. The second case requires only a single light source, where now the bifacial tandem is positioned between two mirrors, perpendicular to each other,

Please cite this article in press as: De Bastiani et al., Bifacial perovskite/silicon tandem solar cells, Joule (2022), https://doi.org/10.1016/j.joule.2022.05.014

at a 45° angle in relation to the device (Figure 5B). At the rear side, intensity filters simulate different rear irradiances together with spectral filters for different effective albedos. For both setups, the main challenge is controlling the sample temperature during the measurements, as conventional temperature-controlled chucks are not suitable here. In our experience, convective cooling with a cold airflow is the best option, even though this can be laborious when measuring devices at different rear irradiances. As bifacial PV is a fast-growing field, equipment suppliers may see opportunities here to offer soon dedicated characterization solutions. Also, certifying bifacial tandem solar cells via independent research institutes will be required, including the establishment of recognized measurement protocols.

POTENTIAL IN THE PV MARKET

Kopecek and Libal exhaustively described in their review entitled "Bifacial Photovoltaics 2021: Status, Opportunities and Challenges" the recent rise of bifacial technology in the c-Si industry.[4] Indeed, the power gain provided by the albedo is rapidly positioning bifacial single-junction c-Si configuration as the leading technology for the lowest levelized cost of electricity (LCOE), in particular at the utility scale. The cumulative installed power capacity of c-Si bifacial systems is growing exponentially, already reaching 20 GW of cumulative capacity in 2020.[4] The International Technology Roadmap for Photovoltaic (ITRPV) thoroughly tracks and updates the expected trends for the main solar technologies every year and acts as a useful reference to understand the global development trends in the solar industry. Figure 6 shows the 2017 and 2021 predictions of the global PV market shares for monofacial and bifacial technologies.[31,62] The growing interest in bifacial technology is exceeding even previous predictions, setting new standards for silicon manufacturing in the near future. The driving force behind this shift in the c-Si PV industry is the gain in power, which translates into a lower LCOE, coupled with improved technologies and a steady reduction in manufacturing costs. Kopecek and Libal's arguments match the new trends in the leading c-Si industries, which are now offering bifacial products among their product portfolios.

For perovskite/silicon tandems, and more generally for perovskite-based technologies, LCOE calculations are still subject to a certain degree of approximation. Aside from the power generation, which can be assumed from scientific publications, the bill-of-material costs are still affected by many assumptions owing to the immature supply chain. To avoid this problem, a common strategy is calculating the average cost per step to fabricate the SHJ bottom cell and using this value to estimate the cost of the additional steps needed to fabricate the tandem cell on a pro rata basis.[63] The degradation rate of the perovskite is even more difficult to take into account. Usually, the best strategy is to assume different degradation rates that are reasonable for a commercial product and from there to calculate different LCOEs. As an example, we report in Figure 6 the ratio between the LCOE of bifacial tandems ($LCOE_{tandem}$) and bifacial single-junction silicon ($LCOE_{silicon}$) technologies for three different cost structures of the tandem (0%, 10% more, and 30% more) and three different perovskite annual degradation rates (0.4%, 2%, and 5%). The details of the LCOE calculations are reported in the supplemental information. For both technologies, we considered a rear-side power gain of 15% due to the albedo. For the silicon, we considered the best product on the market, with an efficiency of 25% (in the presence of the albedo). The trends clearly show the importance of efficiency and stability, compared with the minor role of an increased cost of manufacturing. Moreover, the trends also highlight that improving the stability of tandems is equivalent to or even more important than further enhancing their PCEs, thereby highly supporting the bifacial tandem configuration.

Please cite this article in press as: De Bastiani et al., Bifacial perovskite/silicon tandem solar cells, Joule (2022), https://doi.org/10.1016/j.joule.2022.05.014

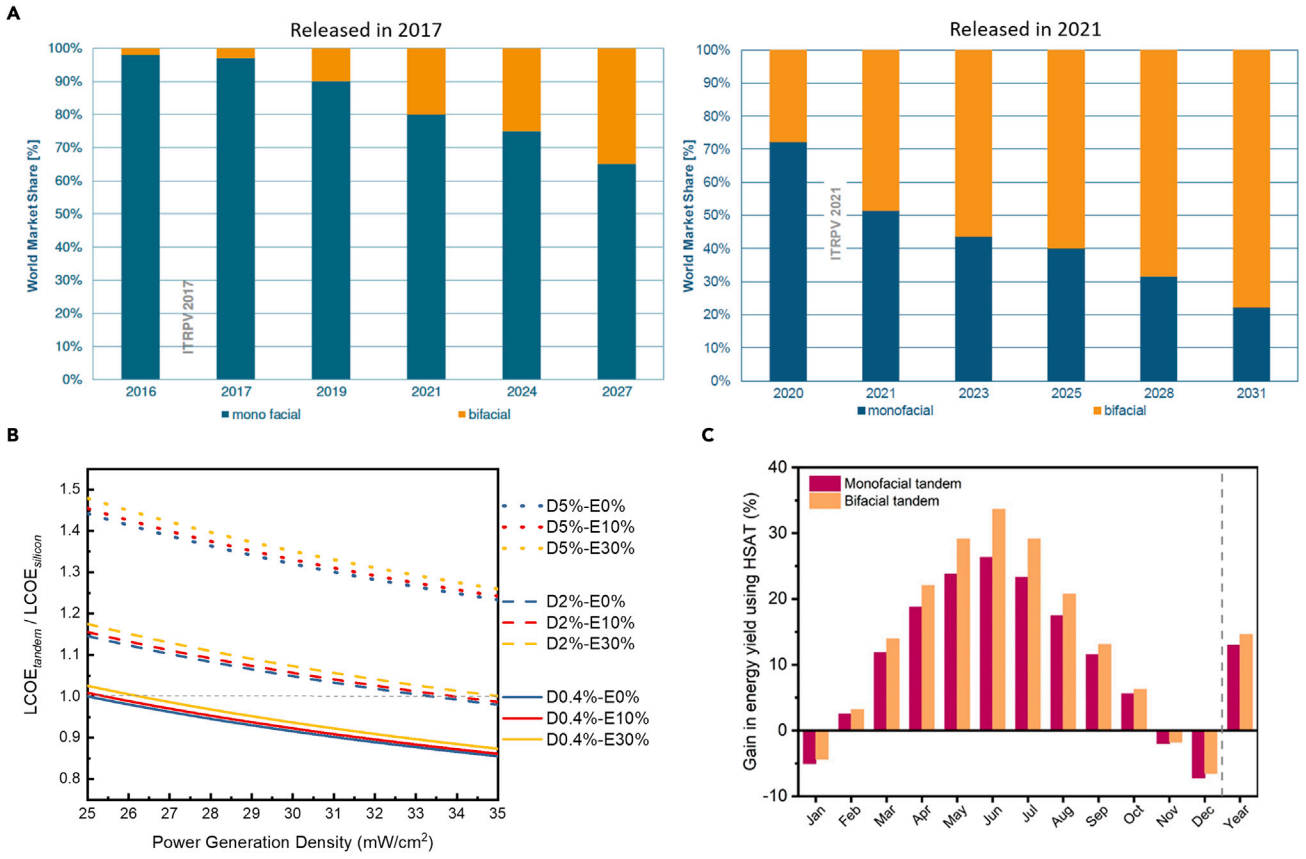

Figure 6. The bifacial photovoltaic market

(A) International Technology Roadmap for Photovoltaic (ITRPV) predictions for monofacial and bifacial technologies in the world market PV share. The left graph reports the predictions foreseen in 2017 and the right graph those of 2021; ITRPV edition and VDMA Photovoltaic Equipment.[31,62]

(B) Ratio between the LCOE of the bifacial tandem and bifacial silicon with a rear-side power gain of 15% for different annual degradation rates (D: 0.4% full line, 2% dashed line, and 5% dotted line) and different cost increments (E: 0% blue, 10% red, and 30% yellow).

(C) Gain in energy yield for a monofacial and a bifacial tandem using a single tracker. Taken from Babics et al.[28]

The gain in power output of a bifacial installation can be further enhanced with tracking technology, as shown in the techno-economic analysis by Peters et al. Indeed, bifacial modules can boost their performance yield by 35% using single-axis tracking, achieving the lowest LCOE for almost any location worldwide.[16] In parallel, such tracked technology allows for a more uniform albedo over the daytime, optimizing the power output of bifacial systems. With single-axis tracking, the bifacial configuration is predicted to become the leading technology in the utility-scale market, driving the transition toward sustainable energy worldwide. Indeed, Babics et al. report a 55% power increment for the tracked tandem with respect to the fixed rack case on a specific day.[28] Moreover, even if the gain in power of the tracked tandem is higher in the summer and negative in winter (based on a specific orientation of the modules and Sun's path), the overall annual boost in performances is as high as 15% (Figure 6). Tracking technology arguably offers the best application for bifacial tandems also because it allows an optimized spacing between the modules and the correct height to maximize the albedo, which are both important to avoid the negative impact of shadowing.[2] Moreover, the albedo may vary over the module itself (due to non-uniform rear albedo or shading from a tracking unit's torque tube) or between modules in a string, and it certainly varies in specific locations during the course of the year (for example, grass in the summer and snow in the winter).

Please cite this article in press as: De Bastiani et al., Bifacial perovskite/silicon tandem solar cells, Joule (2022), https://doi.org/10.1016/j.joule.2022.05.014

Therefore, it is important to foresee a sort of ground management that controls the albedo. This can be done strategically, using highly reflective materials. Overall, these limiting factors clearly point the bifacial tandem toward the utility-scale market, rather than residential applications. Indeed, in rooftop applications, the effect of the albedo is usually minimized by the narrow gap between the roof and the module. For these reasons, we believe that the monofacial configuration (either for tandems or single junctions) will still be the reference technology for the residential PV market.

CONCLUSIONS

Perovskite/silicon tandem technologies are expected to greatly benefit from a bifacial cell architecture, where the enhancement in power output coupled with the improved stability afforded by bifacial perovskite/silicon tandems may be a key driver toward the commercial implementation of perovskite-based solar cells. At the utility scale, we predict that the combination of tandem, bifacial, and tracker technologies will result in a new generation of highly efficient solar farms, ready to deploy electricity toward the terawatt scale. The use of bifacial tandems in conjunction with tracking technology can be a significant driver of perovskite-based tandems in the market, since the advantages in energy yield with single-axis tracking can offset the increased initial costs of the fabrication of new tandem technology, starting perovskite-based solar cells on their path down the experience curve. In both monofacial and bifacial configurations, the initial deployment of perovskite/silicon tandems will be tested on pilot installations in the near future. On the one hand, this will generate more data for reliability and stability analysis and also refine energy yield predictions. On the other hand, it will set the reference for the manufacturing costs of the perovskite, which nowadays is still quite speculative. The success of these pilot tests will be the factor that determines the level of deployment of perovskite-based tandem technologies and whether perovskite/silicon tandems will gradually take over single-junction c-Si technologies in future PV manufacturing.

SUPPLEMENTAL INFORMATION

Supplemental information can be found online at https://doi.org/10.1016/j.joule.2022.05.014.

ACKNOWLEDGMENTS

This work was supported by the King Abdullah University of Science and Technology (KAUST) Office of Sponsored Research (OSR) under award no. OSR-CARF/CCF-3079, OSR-2020-CPF-4519, IED OSR-2019-4208, IED OSR-2019-4580, IED OSR-2020-4611, OSR-CRG2019-4093, and OSR-CRG2020-4350.

AUTHOR CONTRIBUTIONS

M.D.B. and S.D.W. proposed the topic of the work. M.D.B., M.B., E.U., L.X., J.L., E.A., and T.G.A. revised the literature and provided the content. M.D.B. wrote the manuscript. A.S.S. prepared the figures. All the authors revised the manuscript and approved of the final version of the manuscript.

DECLARATION OF INTERESTS

The authors declare no competing interests.

REFERENCES

1. Lin, W., Dréon, J., Zhong, S., Paratte, V., Antognini, L., Cattin, J., Liu, Z., Liang, Z., Gao, P., Shen, H., et al. (2021). Dopant-free bifacial silicon solar cells. Sol. RRL *5*, 2000771.
2. Lehr, J., Langenhorst, M., Schmager, R., Gota, F., Kirner, S., Lemmer, U., Richards, B.S., Case, C., and Paetzold, U.W. (2020). Energy yield of bifacial textured perovskite/silicon tandem photovoltaic modules. Sol. Energy Mater. Sol. Cells *208*, 110367.
3. Asadpour, R., Chavali, R.V.K., Ryyan Khan, M., and Alam, M.A. (2015). Bifacial Si heterojunction-perovskite organic-inorganic tandem to produce highly efficient (η T*$\sim$ 33%) solar cell. Appl. Phys. Lett. *106*, 243902.
4. Kopecek, R., and Libal, J. (2021). Bifacial photovoltaics 2021: status, opportunities and challenges. Energies *14*, 2076.
5. De Bastiani, M., Babics, M., Aydin, E., Subbiah, A.S., Xu, L., and De Wolf, S. (2021). All set for efficient and reliable perovskite/silicon tandem photovoltaic modules? Sol. RRL. *6*, 2100493.
6. Patel, M.T., Ahmed, M.S., Imran, H., Butt, N.Z., Khan, M.R., and Alam, M.A. (2021). Global analysis of next-generation utility-scale PV: tracking bifacial solar farms. Appl. Energy *290*, 116478.
7. Rodríguez-Gallegos, C.D., Liu, H., Gandhi, O., Singh, J.P., Krishnamurthy, V., Kumar, A., Stein, J.S., Li, L., Wang, S., and Reindl, T. (2021). Techno-economic performance modelling of bifacial and tracking PV systems worldwide, 2021 IEEE 48th Photovoltaic Specialists Conference (PVSC) (IEEE Publications), pp. 0406–0409.
8. Hou, Y., Aydin, E., De Bastiani, M., Xiao, C., Isikgor, F.H., Xue, D.J., Chen, B., Chen, H., Bahrami, B., Chowdhury, A.H., et al. (2020). Efficient tandem solar cells with solution-processed perovskite on textured crystalline silicon. Science *367*, 1135–1140.
9. Kim, D., Jung, H.J., Park, I.J., Larson, B.W., Dunfield, S.P., Xiao, C., Kim, J., Tong, J., Boonmongkolras, P., Ji, S.G., et al. (2020). Efficient, stable silicon tandem cells enabled by anion-engineered wide-bandgap perovskites. Science *368*, 155–160.
10. Xu, J., Boyd, C.C., Yu, Z.J., Palmstrom, A.F., Witter, D.J., Larson, B.W., France, R.M., Werner, J., Harvey, S.P., Wolf, E.J., et al. (2020). Triple-halide wide-band gap perovskites with suppressed phase segregation for efficient tandems. Science *367*, 1097–1104.
11. Al-Ashouri, A., Köhnen, E., Li, B., Magomedov, A., Hempel, H., Caprioglio, P., Márquez, J.A., Vilches, A.B.M., Kasparavicius, E., Smith, J.A., et al. (2020). Monolithic perovskite/silicon tandem solar cell with >29% efficiency by enhanced hole extraction. Science *370*, 1300–1309.
12. Sofia, S.E., Wang, H., Bruno, A., Cruz-Campa, J.L., Buonassisi, T., and Peters, I.M. (2020). Roadmap for cost-effective, commercially-viable perovskite silicon tandems for the current and future PV market. Sustainable Energy Fuels *4*, 852–862.
13. Kamaraki, C., Klug, M.T., Green, T., Miranda Perez, L., and Case, C. (2021). Perovskite/silicon tandem photovoltaics: technological disruption without business disruption. Appl. Phys. Lett. *119*, 070501.
14. (NCPV), N.N.C.f.P. (2020). https://www.nrel.gov/pv/cell-efficiency.html.
15. De Bastiani, M., Van Kerschaver, E., Jeangros, Q., Ur Rehman, A., Aydin, E., Isikgor, F.H., Mirabelli, A.J., Babics, M., Liu, J., Zhumagali, S., et al. (2021). Toward stable monolithic perovskite/silicon tandem photovoltaics: a six-month outdoor performance study in a hot and humid climate. ACS Energy Lett. *6*, 2944–2951.
16. Peters, I.M., Hauch, J., Brabec, C., and Sinha, P. (2021). The value of stability in photovoltaics. Joule *5*, 3137–3153.
17. Aydin, E., Allen, T.G., De Bastiani, M., Xu, L., Ávila, J., Salvador, M., Van Kerschaver, E., and De Wolf, S. (2020). Interplay between temperature and bandgap energies on the outdoor performance of perovskite/silicon tandem solar cells. Nat. Energy *5*, 851–859.
18. Hoke, E.T., Slotcavage, D.J., Dohner, E.R., Bowring, A.R., Karunadasa, H.I., and McGehee, M.D. (2015). Reversible photo-induced trap formation in mixed-halide hybrid perovskites for photovoltaics. Chem. Sci. *6*, 613–617.
19. De Bastiani, M., Mirabelli, A.J., Hou, Y., Gota, F., Aydin, E., Allen, T.G., Troughton, J., Subbiah, A.S., Isikgor, F.H., Liu, J., et al. (2021). Efficient bifacial monolithic perovskite/silicon tandem solar cells via bandgap engineering. Nat. Energy *6*, 167–175.
20. De Bastiani, M., Subbiah, A.S., Aydin, E., Isikgor, F.H., Allen, T.G., and De Wolf, S. (2020). Recombination junctions for efficient monolithic perovskite-based tandem solar cells: physical principles, properties, processing and prospects. Mater. Horiz. *7*, 2791–2809.
21. Köhnen, E., Jošt, M., Morales-Vilches, A.B., Tockhorn, P., Al-Ashouri, A., Macco, B., Kegelmann, L., Korte, L., Rech, B., Schlatmann, R., et al. (2019). Highly efficient monolithic perovskite silicon tandem solar cells: analyzing the influence of current mismatch on device performance. Sustainable Energy Fuels *3*, 1995–2005.
22. Aydin, E., Liu, J., Ugur, E., Azmi, R., Harrison, G.T., Hou, Y., Chen, B., Zhumagali, S., De Bastiani, M., Wang, M., et al. (2021). Ligand-bridged charge extraction and enhanced quantum efficiency enable efficient n–i–p perovskite/silicon tandem solar cells. Energy Environ. Sci. *14*, 4377–4390.
23. Isikgor, F.H., Furlan, F., Liu, J., Ugur, E., Eswaran, M.K., Subbiah, A.S., Yengel, E., De Bastiani, M., Harrison, G.T., Zhumagali, S., et al. (2021). Concurrent cationic and anionic perovskite defect passivation enables 27.4% perovskite/silicon tandems with suppression of halide segregation. Joule *5*, 1566–1586.
24. Aydin, E., De Bastiani, M., Yang, X., Sajjad, M., Aljamaan, F., Smirnov, Y., Hedhili, M.N., Liu, W., Allen, T.G., Xu, L., et al. (2019). Zr-doped indium oxide (IZRO) transparent electrodes for perovskite-based tandem solar cells. Adv. Funct. Mater. *29*, 1901741.
25. Mazzarella, L., Lin, Y.H., Kirner, S., Morales-Vilches, A.B., Korte, L., Albrecht, S., Crossland, E., Stannowski, B., Case, C., Snaith, H.J., et al. (2019). Infrared light management using a nanocrystalline silicon oxide interlayer in monolithic perovskite/silicon heterojunction tandem solar cells with efficiency above 25. Adv. Energy Mater. *9*, 1803241.
26. Boccard, M., and Ballif, C. (2020). Influence of the subcell properties on the fill factor of two-terminal perovskite–silicon tandem solar cells. ACS Energy Lett. *5*, 1077–1082.
27. Onno, A., Rodkey, N., Asgharzadeh, A., Manzoor, S., Yu, Z.J., Toor, F., and Holman, Z.C. (2020). Predicted power output of silicon-based bifacial tandem photovoltaic systems. Joule *4*, 580–596.
28. Babics, M., De Bastiani, M., Balawi, A.H., Ugur, E., Aydin, E., Subbiah, A.S., Liu, J., Xu, L., Azmi, R., Allen, T.G., et al. (2022). Unleashing the full power of perovskite/silicon tandem modules with solar trackers. ACS Energy Lett. *7*, 1604–1610.
29. Brennan, M.P., Abramase, A.L., Andrews, R.W., and Pearce, J.M. (2014). Effects of spectral albedo on solar photovoltaic devices. Sol. Energy Mater. Sol. Cells *124*, 111–116.
30. Guerrero-Lemus, R., Vega, R., Kim, T., Kimm, A., and Shephard, L.E. (2016). Bifacial solar photovoltaics–A technology review. Renew. Sustain. Energy Rev. *60*, 1533–1549.
31. ITRPV Edition and VDMA Photovoltaic Equipment (2021). International Technology Roadmap for Photovoltaic, p. 31.
32. Coletti, G., Luxembourg, S.L., Geerligs, L., Rosca, V., Burgers, A., Wu, Y., Okel, L., Kloos, M., Danzl, F., Najafi, M., et al. (2020). Bifacial four-terminal perovskite/silicon tandem solar cells and modules. ACS Energy Lett. *5*, 1676–1680.
33. Song, Z., Chen, C., Li, C., Rijal, S., Chen, L., Li, Y., and Yan, Y. (2021). Assessing the true power of bifacial perovskite solar cells under concurrent bifacial illumination. Sustainable Energy Fuels *5*, 2865–2870.
34. Fu, F., Feurer, T., Jäger, T., Avancini, E., Bissig, B., Yoon, S., Buecheler, S., and Tiwari, A.N. (2015). Low-temperature-processed efficient semi-transparent planar perovskite solar cells for bifacial and tandem applications. Nat. Commun. *6*, 8932.
35. Chen, D., Pang, S., Zhou, L., Li, X., Su, A., Zhu, W., Chang, J., Zhang, J., Zhang, C., and Hao, Y. (2019). An efficient TeO2/Ag transparent top electrode for 20%-efficiency bifacial perovskite solar cells with a bifaciality factor exceeding 80. J. Mater. Chem. A *7*, 15156–15163.
36. Wang, H., Dewi, H.A., Koh, T.M., Bruno, A., Mhaisalkar, S., and Mathews, N. (2020). Bifacial, color-tunable semitransparent perovskite solar cells for building-integrated photovoltaics. ACS Appl. Mater. Interfaces *12*, 484–493.
37. Hanmandlu, C., Chen, C.-Y., Boopathi, K.M., Lin, H.-W., Lai, C.-S., and Chu, C.-W. (2017). Bifacial perovskite solar cells featuring

semitransparent electrodes. ACS Appl. Mater. Interfaces *9*, 32635–32642.

38. Lee, K., Kim, N., Kim, K., Um, H.-D., Jin, W., Choi, D., Park, J., Park, K.J., Lee, S., and Seo, K. (2020). Neutral-colored transparent crystalline silicon photovoltaics. Joule *4*, 235–246.

39. Li, X., Xia, R., Yan, K., Ren, J., Yip, H.-L., Li, C.-Z., and Chen, H. (2020). Semitransparent organic solar cells with vivid colors. ACS Energy Lett. *5*, 3115–3123.

40. Ravishankar, E., Booth, R.E., Saravitz, C., Sederoff, H., Ade, H.W., and O'Connor, B.T. (2020). Achieving net zero energy greenhouses by integrating semitransparent organic solar cells. Joule *4*, 490–506.

41. Sun, C., Xia, R., Shi, H., Yao, H., Liu, X., Hou, J., Huang, F., Yip, H.-L., and Cao, Y. (2018). Heat-insulating multifunctional semitransparent polymer solar cells. Joule *2*, 1816–1826.

42. Rahmany, S., and Etgar, L. (2020). Semitransparent perovskite solar cells. ACS Energy Lett. *5*, 1519–1531.

43. Lim, J.W., Lee, D.J., and Yun, S.J. (2013). Semi-transparent amorphous silicon solar cells using a thin p-Si layer and a buffer layer. ECS Solid State Lett. *2*, Q47–Q49.

44. Liu, J., Aydin, E., Yin, J., De Bastiani, M., Isikgor, F.H., Rehman, A.U., Yengel, E., Ugur, E., Harrison, G.T., Wang, M., et al. (2021). 28.2%-efficient, outdoor-stable perovskite/silicon tandem solar cell. Joule *5*, 3169–3186.

45. Amat, A., Mosconi, E., Ronca, E., Quarti, C., Umari, P., Nazeeruddin, M.K., Grätzel, M., and De Angelis, F. (2014). Cation-induced band-gap tuning in organohalide perovskites: interplay of spin-orbit coupling and octahedra tilting. Nano Lett. *14*, 3608–3616.

46. Konstantakou, M., and Stergiopoulos, T. (2017). A critical review on tin halide perovskite solar cells. J. Mater. Chem. A *5*, 11518–11549.

47. Holman, Z.C., Descoeudres, A., Barraud, L., Fernandez, F.Z., Seif, J.P., De Wolf, S.D., and Ballif, C. (2012). Current losses at the front of silicon heterojunction solar cells. IEEE J. Photovolt. *2*, 7–15.

48. Eperon, G.E., Stranks, S.D., Menelaou, C., Johnston, M.B., Herz, L.M., and Snaith, H.J. (2014). Formamidinium lead trihalide: a broadly tunable perovskite for efficient planar heterojunction solar cells. Energy Environ. Sci. *7*, 982–988.

49. Filip, M.R., Eperon, G.E., Snaith, H.J., and Giustino, F. (2014). Steric engineering of metal-halide perovskites with tunable optical band gaps. Nat. Commun. *5*, 5757.

50. Longo, G., Momblona, C., La-Placa, M.-G., Gil-Escrig, L.n., Sessolo, M., and Bolink, H.J. (2018). Fully vacuum-processed wide band gap mixed-halide perovskite solar cells. ACS Energy Lett. *3*, 214–219.

51. Jesper Jacobsson, T.J., Correa-Baena, J.-P., Pazoki, M., Saliba, M., Schenk, K., Grätzel, M., and Hagfeldt, A. (2016). Exploration of the compositional space for mixed lead halogen perovskites for high efficiency solar cells. Energy Environ. Sci. *9*, 1706–1724.

52. Chen, B., Yu, Z.J., Manzoor, S., Wang, S., Weigand, W., Yu, Z., Yang, G., Ni, Z., Dai, X., Holman, Z.C., et al. (2020). Blade-coated perovskites on textured silicon for 26%-efficient monolithic perovskite/silicon tandem solar cells. Joule *4*, 850–864.

53. Roß, M., Severin, S., Stutz, M.B., Wagner, P., Köbler, H., Favin-Lévêque, M., Al-Ashouri, A., Korb, P., Tockhorn, P., Abate, A., et al. (2021). Co-evaporated formamidinium lead iodide based perovskites with 1000 h constant stability for fully textured monolithic perovskite/silicon tandem solar cells. Adv. Energy Mater. *11*, 2101460.

54. Bush, K.A., Palmstrom, A.F., Yu, Z.J., Boccard, M., Cheacharoen, R., Mailoa, J.P., McMeekin, D.P., Hoye, R.L.Z., Bailie, C.D., Leijtens, T., et al. (2017). 23.6%-efficient monolithic perovskite/silicon tandem solar cells with improved stability. Nat. Energy *2*, 1–7.

55. Zhumagali, S., Isikgor, F.H., Maity, P., Yin, J., Ugur, E., De Bastiani, M., Subbiah, A.S., Mirabelli, A.J., Azmi, R., Harrison, G.T., et al. (2021). Linked nickel oxide/perovskite interface passivation for high-performance textured monolithic tandem solar cells. Adv. Energy Mater. *11*, 2101662.

56. Subbiah, A.S., Isikgor, F.H., Howells, C.T., De Bastiani, M., Liu, J., Aydin, E., Furlan, F., Allen, T.G., Xu, F., Zhumagali, S., et al. (2020). High-performance perovskite single-junction and textured perovskite/silicon tandem solar cells via slot-die-coating. ACS Energy Lett. *5*, 3034–3040.

57. Palmstrom, A.F., Eperon, G.E., Leijtens, T., Prasanna, R., Habisreutinger, S.N., Nemeth, W., Gaulding, E.A., Dunfield, S.P., Reese, M., Nanayakkara, S., et al. (2019). Enabling flexible all-perovskite tandem solar cells. Joule *3*, 2193–2204.

58. Zhao, D., Chen, C., Wang, C., Junda, M.M., Song, Z., Grice, C.R., Yu, Y., Li, C., Subedi, B., Podraza, N.J., et al. (2018). Efficient two-terminal all-perovskite tandem solar cells enabled by high-quality low-bandgap absorber layers. Nat. Energy *3*, 1093–1100.

59. Lin, R., Xiao, K., Qin, Z., Han, Q., Zhang, C., Wei, M., Saidaminov, M.I., Gao, Y., Xu, J., Xiao, M., et al. (2019). Monolithic all-perovskite tandem solar cells with 24.8% efficiency exploiting comproportionation to suppress Sn (ii) oxidation in precursor ink. Nat. Energy *4*, 864–873.

60. Yu, Z., Yang, Z., Ni, Z., Shao, Y., Chen, B., Lin, Y., Wei, H., Yu, Z.J., Holman, Z., and Huang, J. (2020). Simplified interconnection structure based on C60/SnO2-x for all-perovskite tandem solar cells. Nat. Energy *5*, 657–665.

61. Eperon, G.E., Leijtens, T., Bush, K.A., Prasanna, R., Green, T., Wang, J.T.-W., McMeekin, D.P., Volonakis, G., Milot, R.L., May, R., et al. (2016). Perovskite-perovskite tandem photovoltaics with optimized band gaps. Science *354*, 861–865.

62. ITRPV Edition and VDMA Photovoltaic Equipment (2017). International Technology Roadmap for Photovoltaic, p. 35.

63. Razzaq, A., Allen, T.G., Liu, W., Liu, Z., and De Wolf, S. (2022). Silicon heterojunction solar cells: techno-economic assessment and opportunities. Joule *6*, 514–542.